Journal Pre-proof

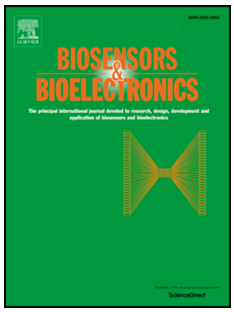

Signal-on electrochemical detection of DNA methylation based on the target-induced conformational change of a DNA probe and exonuclease III-assisted target recycling

Qiumei Feng, Li Qin, Mengying Wang, Po Wang

PII: S0956-5663(19)30926-1

DOI: https://doi.org/10.1016/j.bios.2019.111847

Reference: BIOS 111847

To appear in: *Biosensors and Bioelectronics*

Received Date: 23 August 2019

Revised Date: 29 October 2019

Accepted Date: 2 November 2019

Please cite this article as: Feng, Q., Qin, L., Wang, M., Wang, P., Signal-on electrochemical detection of DNA methylation based on the target-induced conformational change of a DNA probe and exonuclease III-assisted target recycling, *Biosensors and Bioelectronics* (2019), doi: https://doi.org/10.1016/j.bios.2019.111847.

Signal-on electrochemical detection of DNA methylation based on the target-induced conformational change of a DNA probe and exonuclease III-assisted target recycling

Qiumei Feng, Li Qin, Mengying Wang, and Po Wang*

School of Chemistry and Materials Science, Jiangsu Normal University, Xuzhou 221116, China

* Corresponding author

Phone: +86 516 83403165. Fax: +86 516 83536977.

E-mail: wangpo@jsnu.edu.cn (P. Wang).

Abstract

A promising electrochemical system was explored for DNA methylation detection according to the construction of a signal-on biosensor. Based on the ingenious design of probe DNA and auxiliary DNA, methylated target DNA triggered the exonuclease III (Exo III) digestion of auxiliary DNA from 3′-terminus, resulting in the conformational change of probe DNA with an electroactive methylene blue (MB) tag at 5′-terminus. Consequently, the MB tag in the probe DNA was close to the electrode surface for electron transfer, generating an increased current signal. Because of the target recycling of methylated DNA, significant signal amplification was obtained. Moreover, bisulfite conversion conferred an efficient approach for the universal analysis of any CpG sites without the restriction of specific DNA sequence. As a result, the target DNA with different methylation statuses were clearly recognized, and the fully methylated DNA was quantified in a wide range from 10 fM to 100 pM, with a detection limit of 4 fM. The present work realized the assay of methylated target DNA in serum samples with satisfactory results, illustrating the application performance of the system in complex sample matrix.

Keywords: DNA methylation; Electrochemical detection; Conformational change; Signal amplification.

1. Introduction

DNA methylation is an essential component of epigenetic modification associated with many biological processes, such as eukaryote development, cellular differentiation, and gene expression (Jones and Takai, 2001; Jones and Baylin, 2007; Schübeler, 2015; Berney and McGouran, 2018). Aberrant DNA methylation in mammals is associated with various genetic diseases and tumors, including bladder carcinoma, breast cancer, colon tumor, and prostate cancer (Ushijima, 2005). Consequently, accurate and sensitive recognition of DNA methylation is vital for understanding the mechanism of epigenetic regulation of genetic information and molecular pathology for early cancer diagnosis (Wang et al., 2010; Heyn and Esteller, 2012). Restriction enzyme-based detection and bisulfite conversion analysis are two important recognition methods. Restriction enzymes catalyze the scission reaction of unmethylated DNA, while they are limited to analyzing specific base sequences (Zhou et al., 2016). In bisulfite conversion analysis, cytosine is converted to uracil, whereas methylated cytosine remains unchanged in any DNA sequence (Feng et al., 2008). Therefore, bisulfite conversion analysis can expand the scope of the detection target for DNA methylation analysis (Kato et al., 2011).

Electrochemical detection methods are simple, fast, selective, and suitable for real-time *in situ* assays, and have thus attracted substantial attention for analyzing DNA methylation (Kato et al., 2008; Tanaka et al., 2007; Feng et al., 2019; Liu et al., 2011; Li et al., 2012; Tsutsui et al., 2011; Wang et al., 2013; Wang et al., 2015; Gao et al., 2018). For example, Muren and Barton developed a multiplexed chip platform for a robust, nonradioactive assay of bacterial and human methyltransferase activity

(Muren and Barton, 2013). Moreover, an innovative secondary electrode array sensing system was designed for analyzing colorectal tumor tissue based on low-density DNA monolayer patterning and DNA charge transport (Furst et al., 2014). Interestingly, Kurita et al. reported the on-chip evaluation of cytosine methylation level in genomic DNA using an excellent nanocarbon film electrode with nanocrystalline structure (Kurita et al., 2017). We used bisulfite conversion to develop a label-free electrochemical biosensor for profiling the methylation information of the p53 gene according to the current signal of a $[Ru(NH_3)_6]^{3+}$ indicator (Wang et al., 2012). Recently, the methylation status of a tumor suppressor gene was assessed rapidly in human serum and tissue samples with elegant results using immunomagnetic beads (Povedano et al., 2018). Although these approaches obtained DNA methylation information, the improvement of sensitivity is highly required because DNA samples are tiny in many diagnostic scenarios.

An electrochemical DNA (E-DNA) sensor based on the hybridization-induced conformational change of a redox-tagged stem-loop DNA probe has been developed for bioassays (Xiao et al., 2007a; Xiao et al., 2007b). Compared with cumbersome traditional sensors, the E-DNA sensor provided a convenient, reagentless, and single-step DNA detection method (Xiao et al., 2005; Xiao et al., 2006), which was suitable for real-world oligonucleotide detection. Fan et al. pioneered a signal-off E-DNA sensor for the sequence-specific detection of DNA, in which target binding reduced the redox current (Fan et al., 2003). Ricci et al. confirmed that the E-DNA signal arose from the hybridization-linked conformational change, which altered the

electron transfer efficiency between the redox moiety and the electrode surface (Ricci et al., 2007). However, these methods suffered from limited signal gain; no more than 100% of the original current could be obtained. Moreover, surrounding contaminants also produced false positives, which were difficult to distinguish from the signal change arising from the intended target (Xiao et al., 2005; Cash et al., 2009). In consideration of the above problems from signal-off E-DNA system, it is necessary to design a signal-on E-DNA sensor, which can increase the signal response after target recognition.

To achieve a highly sensitive electrochemical biosensing system, various amplification strategies have been explored, such as polymerase chain reaction (PCR) (Clark et al., 2006; Burke et al., 2009), hybridization chain reaction (HCR) (Chen et al., 2019), DNA structure-based assembly (Li et al., 2013; Zhou et al., 2017), and rolling circle amplification (RCA) (Bi et al., 2013; Gao et al., 2017). These recycling amplification systems are mainly used for recycling probes, signals, and targets. Target regeneration is a promising recycling amplification strategy, in which a single target could produce multiple binding events. For example, exonuclease III (Exo III)-assisted target recycling amplification allowed the recognition of the blunt 3′-terminus of a molecular beacon in a double-stranded DNA probe and the selective digestion of a molecular beacon (Zuo et al., 2010; Xiong et al., 2015). Consequently, the autonomous generation of target DNA allowed continuous hybridization, resulting in higher sensitivity and a lower detection limit.

In this work, we developed a signal-on E-DNA biosensor sensitized with Exo III-assisted recycling strategy for analyzing DNA methylation. In this approach, one terminus of the stem-loop probe DNA was modified with a thiol group that bound chemically to the Au nanoparticles (nano-Au) modified electrode via an Au–S bond. The other terminus was covalently modified with a methylene blue (MB) tag. After the introduction of auxiliary DNA, the stem-loop structure of the probe DNA opened to form double-stranded probe DNA/auxiliary DNA with a rod-like structure, sequestering MB from the electrode surface, and exhibiting a lower current signal. The methylated cytosine in target DNA remained unchanged after the treatment of bisulfite. Hence, upon the addition of methylated target DNA, probe DNA/auxiliary DNA/methylated target DNA complex was formed through complementary hybridization. With the help of Exo III, the auxiliary DNA was digested from the 3′-terminus, and the released methylated target DNA would hybridize with another auxiliary DNA. The continuous hybridization of methylated target DNA constantly triggered digestion, resulting in large signal amplification. Consequently, the stem-loop structure of the probe DNA was regenerated, and the rate at which the MB tag hit the electrode surface was improved, increasing the electron transfer and Faradic current (“signal-on” status). Therefore, based on the target-induced conformational change of the MB tag-bound probe DNA, signal transduction for methylated target DNA analysis with a detectable increase in redox current was achieved.

2. Experimental

118 *2.1. Reagents and apparatus*

119 Trihydrate chloroauric acid ($HAuCl_4 \cdot 3H_2O$), tris(2-carboxyethyl) phosphine
120 hydrochloride (TCEP), $K_3[Fe(CN)_6]$, and $K_2[Fe(CN)_6]$ were obtained from
121 Sigma-Aldrich (St. Louis, MO, USA), and used without further purification. Exo III
122 was purchased from Takara Biotechnology Co., Ltd (Dalian, China). Phosphate
123 buffered solution (PBS; pH 7.4) was prepared by mixing stock solutions of 0.1 M
124 KH_2PO_4, Na_2HPO_4, and NaCl. Unless otherwise stated, all reagents were of analytical
125 grade, and all aqueous solutions were prepared with ultrapure water obtained from a
126 Millipore water purification system (resistivity $\geq$ 18.2 MΩ·cm). All sequences of
127 oligonucleotides from Sangon Biological Engineering Technology and Services Co.,
128 Ltd. (Shanghai, China) were listed in Table S1.

129 All electrochemical measurements, including differential pulse voltammetry
130 (DPV), cyclic voltammetry (CV), and electrochemical impedance spectroscopy (EIS),
131 were performed on a CHI 660E electrochemical workstation (Chenhua, Shanghai,
132 China) at room temperature. A conventional three-electrode cell was used in all
133 experiments, in which a bare or modified glassy carbon electrode (GCE), a
134 silver/silver chloride electrode, and a platinum wire served as a working electrode,
135 reference electrode, and counter electrode, respectively.

136 *2.2. Electrode preparation and modification*

137 Prior to surface modification, the GCE was polished with 1.0, 0.3, and 0.05 μm
138 alumina slurries, followed by successive sonication in ethanol and ultrapure water for

5 min. After cleaning, the nano-Au film was deposited *in situ* on the GCE surface by a CV scan from 0.20 to –1.0 V in pH 7.4 PBS containing 0.25 mg mL^{-1} $HAuCl_4$ at 50 mV s^{-1} for 12 cycles. Subsequently, the resulting electrode was incubated with 100 μL of 1 μM probe DNA at 4 °C overnight to graft probe DNA onto the electrode surface through Au–S bonds. Before incubation, the thiolated probe DNA was activated by 10 mM TCEP to break the S–S bond, followed by purification with a Millipore centrifugal filter to remove the excess TCEP. After rinsing, the probe DNA/nano-Au/GCE was submerged in 100 μL of 1 μM auxiliary DNA, yielding auxiliary DNA/probe DNA/nano-Au/GCE.

2.3. Analytical procedure

The auxiliary DNA/probe DNA/nano-Au/GCE was submerged in 100 μL of 10 mM Tris-HCl solution (pH 8.0, 50 mM NaCl, 10 mM $MgCl_2$) containing 0.4 unit μL^{-1} Exo III and target DNA with different methylation statuses for 2 h. Then, the target DNA recycling amplification was triggered. According to our previous work (Wang et al., 2012), the target DNA was treated with bisulfite to convert unmethylated cytosine to uracil before incubation. Finally, after rinsing thoroughly, the sensing interface as an electrochemical biosensor was detected in 0.1 M pH 7.4 PBS under a nitrogen atmosphere. To record the electrochemical response, DPV was performed from –0.8 to 0.2 V with the following experimental parameters: amplitude, 50 mV; pulse width, 0.05 s; sampling width, 0.0167 s; and pulse period, 0.2 s.

3. Results and discussion

3.1. Construction of the signal-on E-DNA sensor

Scheme 1 shows schematics of the construction of the electrochemical sensing platform, the Exo III-assisted target recycling amplification, and the target-induced conformational change of the electrode-bound oligonucleotides. The stem-loop structural probe DNA modified with a thiol group at the 3′ end was immobilized on the nano-Au modified GCE via an Au–S bond. The probe had an MB tag at the 5′ end. Upon hybridization with complementary auxiliary DNA, the stem-loop structure of the probe DNA was broken, and a rigid double-stranded conformation was formed between the probe DNA and one terminus of the auxiliary DNA. Single-stranded DNA formed from the other terminus of the auxiliary DNA. Thus, there was a large distance between the MB tag and the electrode surface, reducing electron transfer efficiency, and decreasing the apparent Faradic current. For target DNA with different methylation states, bisulfite treatment converted unmethylated cytosine to uracil, leaving methylated cytosine intact (Feng et al., 2008). The methylated target DNA hybridized with the remaining single-stranded segment of auxiliary DNA, forming a probe DNA/auxiliary DNA/target DNA complex. It was proved that Exo III could selectively cleave double-stranded DNA from the 3′-OH blunt or recessed end, and showed limited activity for the 3′-overhang end of double-stranded DNA or single-stranded DNA (Zuo et al., 2010; Xiong et al., 2015). In the present study, Exo III cleaved and digested the complex on the electrode surface from the 3′-OH blunt end of the auxiliary DNA. After digestion, the target DNA spontaneously dissociated from the probe DNA/auxiliary DNA/target DNA complex, and then the dissociated

target DNA was reused in the next reaction cycles. Based on Watson-Crick base-pair behavior, the stem-loop structure of the probe DNA was reformed again, forcing the redox tag into close proximity with the electrode surface. After sufficient signal amplification, the rate at which the redox tag (MB) hit the electrode surface was increased, resulting in efficient electron transfer and an increase in the apparent Faradic current. In contrast, for unmethylated DNA, the Exo III cleavage activity was much lower for the mismatched DNA structure, and the MB tag was further from the electrode surface, resulting in a weak current response.

Scheme 1

3.2. Electrochemical characteristics of the signal-on E-DNA sensor

CV and EIS were employed to characterize the stepwise modification of an electrode surface with a $[Fe(CN)_6]^{3-/4-}$ probe. The diameter of the high-frequency semicircle can be used to evaluate the interfacial charge transfer resistance (R_{ct}), which controlled the electron transfer kinetics of the redox reaction at the electrode surface. As shown in Fig. 1, compared with bare GCE (curve a), nano-Au/GCE (curve b) presented an increase in peak current in CV and an almost straight line with much lower resistance in EIS. These results were explained by the high conductivity of nano-Au (see Fig. S1 for morphological characterization), which increased the electron transfer rate and increased the effective area of the electrode. The successive assembly of probe DNA (curve c) and auxiliary DNA (curve d) on nano-Au/GCE decreased the current signal and increased the R_{ct} value owing to the electrostatic

repulsion between the electroactive $[Fe(CN)_6]^{3-/4-}$ probe and the negatively charged DNA backbone. Nevertheless, after further treatment with methylated target DNA in the presence of Exo III (curve e), the CV signal increased dramatically, and the R_{ct} value decreased simultaneously. The continuous cleavage process in the Exo III-assisted target DNA recycling digested the auxiliary DNA into mononucleotides, which was accompanied by a decrease in the negative charge of the electrode interface. Therefore, the interface charge transfer was increased. The CV measurements and EIS responses confirmed that the sensor was fabricated as intended.

Fig. 1

3.3. Feasibility of the signal-on E-DNA sensor

To verify the feasibility of the signal-on E-DNA sensor for analyzing DNA methylation status, methylated DNA and wild type DNA without methylation were assayed. As shown in Fig. 2A, in the presence of complementary methylated target DNA (curve a), the peak current was much higher than that of wild type DNA (curve b). The hybridization of methylated target DNA triggered the selective cleavage and digestion of the double-stranded DNA from the 3′-OH blunt terminus of auxiliary DNA, resulting in the regeneration of hairpin structure in the probe DNA. Thus, the MB-modified end of the probe DNA was close to the electrode surface, producing up to a 4.6-fold increase in redox current.

Fig. 2

224 To validate the Exo III-assisted target recycling amplification strategy, a series of
225 control experiments were performed. As shown in Fig. 2B, a well-defined DPV peak
226 was observed in the presence of target DNA and Exo III (curve a). However, in the
227 absence of Exo III (curve b) or target DNA (curve c), weak DPV responses were
228 obtained, which were similar to that of auxiliary DNA/probe DNA/nano-Au/GCE
229 treated only with Tris-HCl solution (curve d). These results indicated that the
230 methylated target DNA triggered cleavage by Exo III, and the signal-on E-DNA
231 sensor was suitable for analyzing target DNA.

232 *3.4. Recognition of methylation sites*

233 An important challenge in the DNA methylation assay was the identification of
234 methylation position. Therefore, the recognition behavior of the signal-on E-DNA
235 sensor was investigated by measuring the peak current responses to a series of DNA
236 sequences with different methylation sites. The DNA sequences with different
237 methylation status, including unmethylated target DNA, fully methylated target DNA,
238 head hemimethylated target DNA, and middle hemimethylated target DNA, were
239 pretreated with bisulfite. As depicted in Fig. 3, unmethylated target DNA exhibited a
240 weak current signal (curve a), whereas the highest peak current was observed for
241 hybridization with the fully methylated target DNA (curve b). Compared with
242 unmethylated target DNA, the peak current increased slightly for head
243 hemimethylated target DNA (curve c), and the middle hemimethylated target DNA
244 showed only a small current change (curve d). In particular, the peak current in curve

245 c (mC in the head of the sequence) was higher than that of curve d (mC in the middle
246 of the sequence), because a mismatch in the middle of the target DNA has a greater
247 effect on the duplex stability (Wang et al., 2012). These results indicated that the
248 signal-on E-DNA sensor selectively recognized the methylation site of the target
249 DNA.

250 **Fig. 3**

251 *3.5. Optimization of Exo III concentration and reaction time*

252 To improve the detection sensitivity, the experimental conditions were optimized.
253 Fig. 4A shows the effect of Exo III concentration on the current response for the
254 detection of 50 pM methylated target DNA. The current signal increased with the
255 increase in Exo III concentration, and reached a plateau at 0.4 unit μL^{-1}. The result of
256 a time-course experiment for the Exo III-assisted recycling amplification time is
257 presented in Fig. 4B. The current signal increased with the increase in Exo III reaction
258 time before 120 min. The continuously increasing current signal demonstrated that
259 Exo III-assisted autocatalytic target recycling is feasible. Thus, the optimal Exo III
260 concentration of 0.4 unit μL^{-1} and autocatalytic reaction time of 120 min were chosen
261 for further analytical experiments.

262 **Fig. 4**

263 *3.6. Analytical applications*

The sensing behavior of the signal-on E-DNA sensor for methylated DNA detection was measured under the optimal experimental conditions. As shown in Fig. 5A, the peak current of MB increased with the increase in the concentration of methylated target DNA. The increase in peak current ($\Delta I = I - I_0$, where I and I_0 are the electrochemical responses of the signal-on E-DNA sensor in the presence and absence of methylated target DNA, respectively) showed a linear relationship with the logarithmic value of the methylated target DNA concentration ranging from 10 fM to 100 pM, with a correlation coefficient of 0.997 (Fig. 5B). The limit of detection (LOD) was calculated to be 4 fM based on the equation LOD = 3S/m, where S is the standard deviation of blank determinations and m is the slope of calibration curve (Radi et al., 2006; Miao et al., 2018; Labib et al., 2012; Wang et al., 2017). This result was attributed to the excellent physicochemical properties of nano-Au and the Exo III-assisted target recycling amplification strategy. Moreover, the relative standard deviation of six independently fabricated sensors for the detection of 50 pM methylated target DNA was 4.2%, indicating acceptable precision and fabrication reproducibility. Table S2 lists the analytical parameters for the DNA methylation assay of the signal-on E-DNA sensor and reference works (Huertas et al., 2018; Luo et al., 2019; Jiang et al., 2018; Sotgia et al., 2010; Sui et al., 2019; Sadeghan et al., 2018; Zhu et al., 2013; Povedano et al., 2019; Daneshpour et al., 2016; Dai et al., 2013; Hong et al., 2018). The signal-on E-DNA sensor had a relatively lower LOD and wider dynamic concentration response range.

Fig. 5

To evaluate the practical application of the signal-on E-DNA sensor in a complex sample matrix, a recovery test was performed by spiking 20% human blood serum with fully methylated target DNA to simulate a real sample. The human blood serum samples were provided by healthy volunteers in Xuzhou Central Hospital in Jiangsu Province, China. For samples spiked with 100 fM, 1 pM, and 10 pM fully methylated target DNA, the recoveries were 95.6%, 103.5%, and 97.2%, respectively, demonstrating high selectivity and suitability of the signal-on E-DNA sensor for real sample analysis.

3.7. Interference investigation

To investigate the influences of interferences on the assay of target DNA, a variety of foreign substances were added into 50 pM methylated target DNA for electrochemical detection. It was revealed that 100-fold concentration of the following ions exhibited negligible interferences on the determination (signal variations < 3%): Na^+, Ca^{2+}, K^+, Cu^{2+}, Fe^{3+}, Cl^-, HCO_3^-, $H_2PO_4^-$, NO_3^-, and SO_4^{2-}. The effects of some proteins and electroactive biological molecules were also tested. The results indicated that the current changes of MB were lower than 5% of the original signal after the introduction of 50-fold concentration of hemoglobin, thrombin, and telomerase. Although electroactive molecules of dopamine, uric acid, and norepinephrine could be oxidized at the sensing interface, their oxidation potentials were far from the reduction potential of MB, resulting in no significant interfere behavior in a 100-fold concentration (signal changes < 5%).

4. Conclusions

We proposed a signal-on electrochemical biosensing platform for sensitive recognition and detection of DNA methylation. In light of bisulfite conversion, the DNA methylation information was translated into nucleic acid sequence information, which provided a promising strategy for the hybridization detection of target DNA methylation. With the assistance of auxiliary DNA, the Exo III-based recycling amplification was triggered by target DNA hybridization, causing the conformational rearrangement of probe DNA from a rod-like to a stem-loop structure. As a result, the redox tag was forced into close proximity with the electrode surface, facilitating efficient electron transfer, and generating a large increase in the observed Faradic current. Owing to the Exo III-assisted target recycling, the signal-on E-DNA sensor exhibited high sensitivity for methylated target DNA detection, even when challenged with human blood serum. Moreover, specific methylation sites in the DNA sequence were clearly recognized due to the difference of the methylated positions in the molecular structure. Compared with the analytical parameters of various reference methods, the present assay had a relatively wider linear range and lower LOD, indicating the advantages and effectiveness of the biosensing system.

Acknowledgements

This work was financially supported by the National Natural Science Foundation of China (Nos. 21705062 and 21675067), the Natural Science Foundation of Jiangsu Province (Nos. BE2019645 and BK20170228), and the Natural Science Foundation of Xuzhou City (No. KC19161).

References

Berney, M., McGouran, J.F., 2018. Nat. Rev. Chem. 2, 332−348.

Bi, S., Zhao, T., Luo, B., Zhu, J.J., 2013. Chem. Commun. 49, 6906−6908.

Burke, D.G., Griffiths, K., Kassir, Z., Emslie, K., 2009. Anal. Chem. 81, 7294−7301.

Cash, K.J., Heeger, A.J., Plaxco, K.W., Xiao, Y., 2009. Anal. Chem. 81, 656−661.

Chen, X., Huang, J., Zhang, S., Mo, F., Su, S., Li, Y., Fang, L., Deng, J., Huang, H., Luo, Z., Zheng, J., 2019. ACS Appl. Mater. Interfaces 11, 3745−3752.

Clark, S.J., Statham, A., Stirzaker, C., Molloy, P.L., Frommer, M., 2006. Nat. Protoc. 1, 2353−2364.

Dai, Z., Cai, T., Zhu, W., Gao, X., Zou, X., 2013. Chem. Commun. 49, 1939−1941.

Daneshpour, M., Moradi, L.S., Izadi, P., Omidfar, K., 2016. Biosens. Bioelectron. 77, 1095−1103.

Fan, C., Plaxco, K.W., Heeger, A.J., 2003. Proc. Natl. Acad. Sci. U. S. A. 100, 9134−9137.

Feng, F., Wang, H., Han, L., Wang, S., 2008. J. Am. Chem. Soc. 130, 11338−11343.

Feng, Q., Wang, M., Qin, L., Wang, P., 2019. ACS Sens. 4, 2615−2622.

Furst, A.L., Muren, N.B., Hill, M.G., Barton, J.K., 2014. Proc. Natl. Acad. Sci. U. S. A. 111, 14985−14989.

Gao, F., Fan, T., Ou, S., Wu, J., Zhang, X., Luo, J., Li, N., Yao, Y., Mou, Y., Liao, X., Geng, D., 2018. Biosens. Bioelectron. 99, 201−208.

Gao, F., Zhou, F., Chen, S., Yao, Y., Wu, J., Yin, D., Geng, D., Wang, P., 2017. Analyst 142, 4308−4316.

Heyn, H., Esteller, M., 2012. Nat. Rev. Genet. 13, 679−692.

Hong, S.A., Kim, Y.J., Kim, S.J., Yang, S., 2018. Biosens. Bioelectron. 107, 103−110.

Huertas, C.S., Aviñó, A., Kurachi, C., Piqué, A., Sandoval, J., Eritja, R., Esteller, M., Lechuga, L.M., 2018. Biosens. Bioelectron. 120, 47−54.

Jiang, W., Yin, H., Zhou, Y., Duan, J., Li, H., Wang, M., Waterhouse, G.I.N., Ai, S., 2018. Sens. Actuators B 274, 144−151.

Jones, P.A., Baylin, S.B., 2007. Cell 128, 683−692.

Jones, P.A., Takai, D., 2001. Science 293, 1068−1070.

Kato, D., Goto, K., Fujii, S., Takatsu, A., Hirono, S., Niwa, O., 2011. Anal. Chem. 83, 7595−7599.

Kato, D., Sekioka, N., Ueda, A., Kurita, R., Hirono, S., Suzuki, K., Niwa, O., 2008. J. Am. Chem. Soc. 130, 3716−3717.

Kurita, R., Yanagisawa, H., Kamata, T., Kato, D., Niwa, O., 2017. Anal. Chem. 89, 5976−5982.

Labib, M., Zamay, A.S., Muharemagic, D., Chechik, A.V., Bell, J.C., Berezovski, M.V., 2012. Anal. Chem. 84, 2548−2556.

Li, W., Wu, P., Zhang, H., Cai, C., 2012. Anal. Chem. 84, 7583−7590.

Li, Y., Luo, X., Yan, Z., Zheng, J., Qi, H., 2013. Chem. Commun. 49, 3869−3871.

Liu, S., Wu, P., Li, W., Zhang, H., Cai, C., 2011. Chem. Commun. 47, 2844−2846.

Luo, X., Jiang, L., Kang, T., Xing, Y., Zheng, E., Wu, P., Cai, C., Yu, Q., 2019. Anal. Chem. 91, 7304−7312.

Miao, X., Cheng, Z., Ma, H., Li, Z., Xue, N., Wang, P., 2018. Anal. Chem. 90,

1098−1103.

Muren, N.B., Barton, J.K., 2013. J. Am. Chem. Soc. 135, 16632−16640.

Povedano, E., Montiel, V.R.V., Valverde, A., Navarro-Villoslada, F., Yáñez-Sedeño, P., Pedrero, M., Montero-Calle, A., Barderas, R., Peláez-García, A., Mendiola, M., Hardisson, D., Feliú, J., Camps, J., Rodríguez-Tomàs, E., Joven, J., Arenas, M., Campuzano, S., Pingarrón, J.M., 2019. ACS Sens. 4, 227−234.

Povedano, E., Valverde, A., Montiel, V.R.V., Pedrero, M., Yáñez-Sedeño, P., Barderas, R., Segundo-Acosta, P.S., Peláez-García, A., Mendiola, M., Hardisson, D., Campuzano, S., Pingarrón, J.M., 2018. Angew. Chem. Int. Ed. 57, 8194−8198.

Radi, A., Sánchez, J.L.A., Baldrich, E., O′Sullivan, C.K., 2006. J. Am. Chem. Soc. 128, 117−124.

Ricci, F., Lai, R.Y., Plaxco, K.W., 2007. Chem. Commun. 36, 3768−3770.

Sadeghan, A.A., Soltaninejad, H., Hosseinkhani, S., Hosseini, M., Ganjali, M.R., Asadollahi, M.A., 2018. Anal. Chim. Acta 1038, 157−165.

Schübeler, D., 2015. Nature 517, 321−326.

Sotgia, S., Zinellu, A., Pisanu, E., Murgia, L., Pinna, G.A., Gaspa, L., Deiana, L., Carru, C., 2010. Anal. Bioanal. Chem. 396, 2937−2941.

Sui, C., Wang, T., Zhou, Y., Yin, H., Meng, X., Zhang, S., Waterhouse, G.I.N., Xu, Q., Zhuge, Y., Ai, S., 2019. Biosens. Bioelectron. 127, 38−44.

Tanaka, K., Tainaka, K., Kamei, T., Okamoto, A., 2007. J. Am. Chem. Soc. 129, 5612−5620.

Tsutsui, M., Matsubara, K., Ohshiro, T., Furuhashi, M., Taniguchi, M., Kawai, T.,

2011. J. Am. Chem. Soc. 133, 9124−9128.

Ushijima, T., 2005. Nat. Rev. Cancer 5, 223−231.

Wang, P., Chen, H., Tian, J., Dai, Z., Zou, X., 2013. Biosens. Bioelectron. 45, 34−39.

Wang, P., Han, P., Dong, L., Miao, X., 2015. Electrochem. Commun. 61, 36−39.

Wang, P., Mai, Z., Dai, Z., Zou, X., 2010. Chem. Commun. 46, 7781−7783.

Wang, P., Wang, M., Zhou, F., Yang, G., Qu, L., Miao, X., 2017. Electrochem. Commun. 81, 74−78.

Wang, P., Wu, H., Dai, Z., Zou, X., 2012. Chem. Commun. 48, 10754−10756.

Xiao, Y., Lai, R.Y., Plaxco, K.W., 2007a. Nat. Protoc. 2, 2875−2880.

Xiao, Y., Lubin, A.A., Baker, B.R., Plaxco, K.W., Heeger, A.J., 2006. Proc. Natl. Acad. Sci. U. S. A. 103, 16677−16680.

Xiao, Y., Piorek, B.D., Plaxco, K.W., Heeger, A.J., 2005. J. Am. Chem. Soc. 127, 17990−17991.

Xiao, Y., Qu, X., Plaxco, K.W., Heeger, A.J., 2007b. J. Am. Chem. Soc. 129, 11896−11897.

Xiong, E., Zhang, X., Liu, Y., Zhou, J., Yu, P., Li, X., Chen, J., 2015. Anal. Chem. 87, 7291−7296.

Zhou, F., Yao, Y., Luo, J., Zhang, X., Zhang, Y., Yin, D., Gao, F., Wang, P., 2017. Anal. Chim. Acta 969, 8−17.

Zhou, H., Han, T., Wei, Q., Zhang, S., 2016. Anal. Chem. 88, 2976−2983.

Zhu, G., Yang, K., Zhang, C.Y., 2013. Biosens. Bioelectron. 49, 170−175.

Zuo, X., Xia, F., Xiao, Y., Plaxco, K.W., 2010. J. Am. Chem. Soc. 132, 1816−1818.

Captions and Legends

Scheme 1. Schematic illustration of the signal-on E-DNA sensor for DNA methylation detection based on the target-induced conformational change of the DNA probe and Exo III-assisted target recycling.

Fig. 1. (A) CV curves and (B) EIS plots recorded at different stages of the working electrode in 5 mM $[Fe(CN)_6]^{3-/4-}$ containing 0.1 M KCl: bare GCE (a); nano-Au/GCE (b); probe DNA/nano-Au/GCE (c); auxiliary DNA/probe DNA/nano-Au/GCE (d); and auxiliary DNA/probe DNA/nano-Au/GCE incubated with 10 mM Tris-HCl solution containing 0.4 unit μL^{-1} Exo III and 50 pM target DNA (e).

Fig. 2. (A) Background-subtracted DPV responses of the auxiliary DNA/probe DNA/nano-Au/GCE incubated with Tris-HCl solution containing 0.4 unit μL^{-1} Exo III and 50 pM methylated target DNA (a) and 50 pM wild type unmethylated target DNA (b). (B) Background-subtracted DPVs obtained upon analyzing 50 pM methylated target DNA in the presence of 0.4 unit μL^{-1} Exo III (curve a). Curves b to d: control experiments performed with no Exo III (b), no methylated target DNA (c), and no methylated target DNA or Exo III (d).

Fig. 3. Background-subtracted DPVs of the signal-on E-DNA sensor for the analysis of 1 pM unmethylated target DNA (a), fully methylated target DNA (b), head hemimethylated target DNA (c), and middle hemimethylated target DNA (d).

Fig. 4. Effects of (A) Exo III concentration and (B) Exo III-assisted autocatalytic recycling time on the DPV responses toward 50 pM methylated target DNA.

Fig. 5. (A) Background-subtracted DPVs of the signal-on E-DNA sensor for the detection of methylated target DNA at 10 fM (a), 100 fM (b), 500 fM (c), 1 pM (d), 10 pM (e), 50 pM (f), and 100 pM (g). (B) Linear relationship between the current increment and the logarithm of the methylated target DNA concentration.

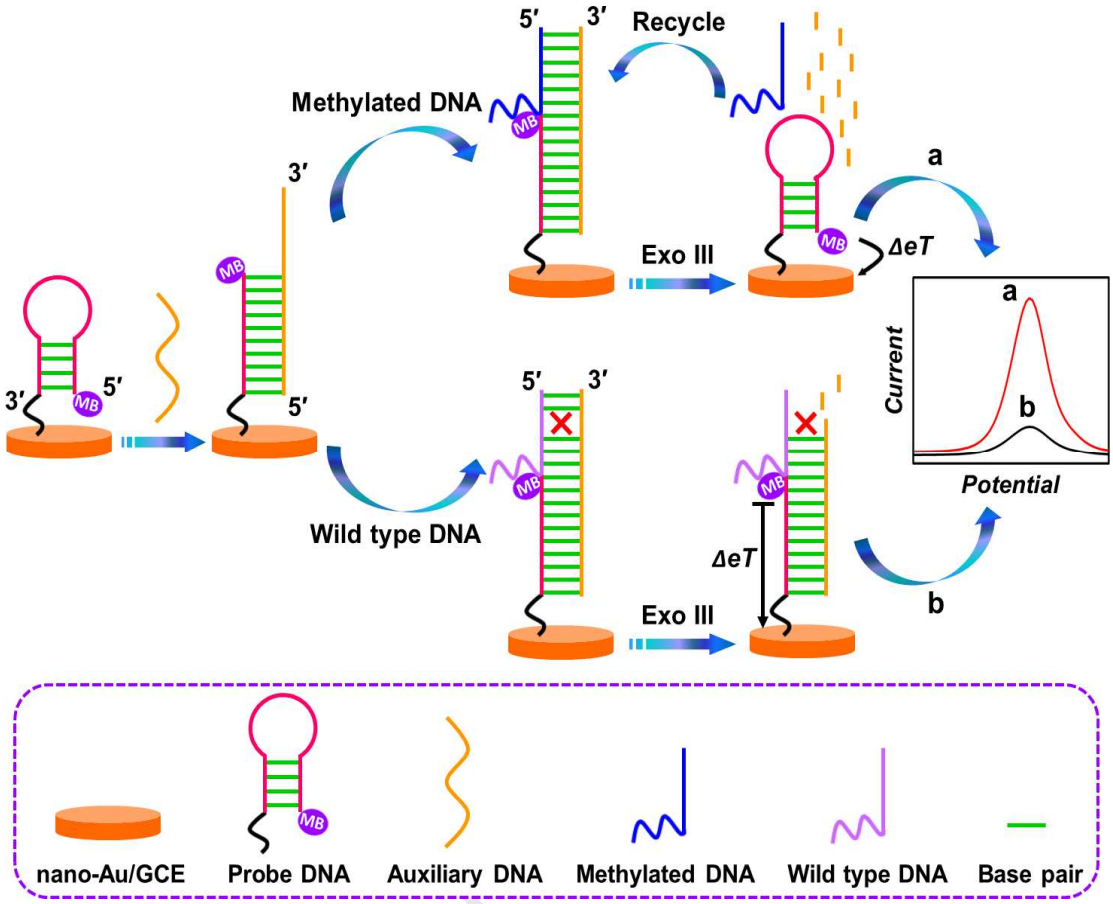

Scheme 1

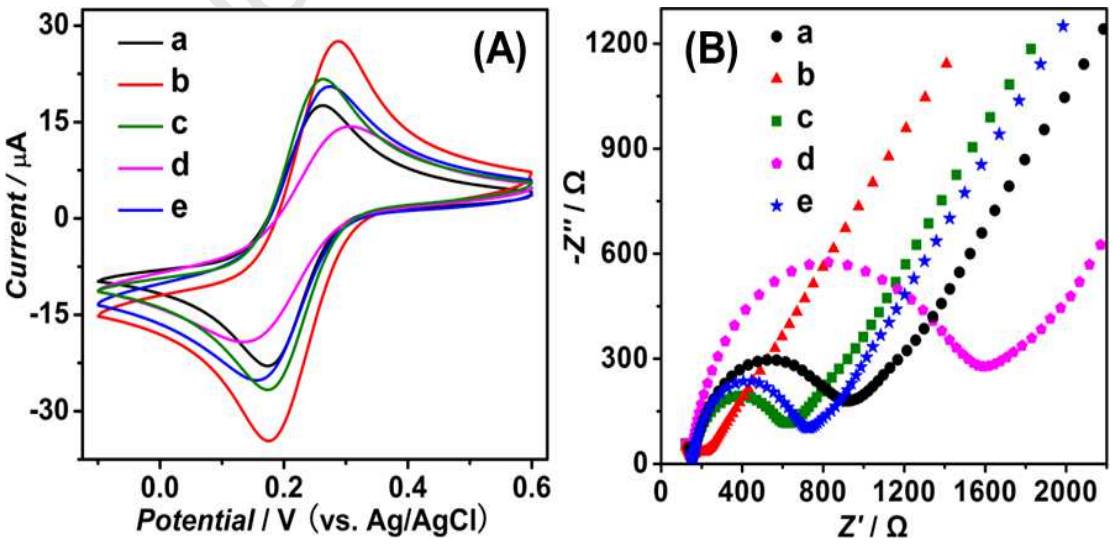

Fig. 1

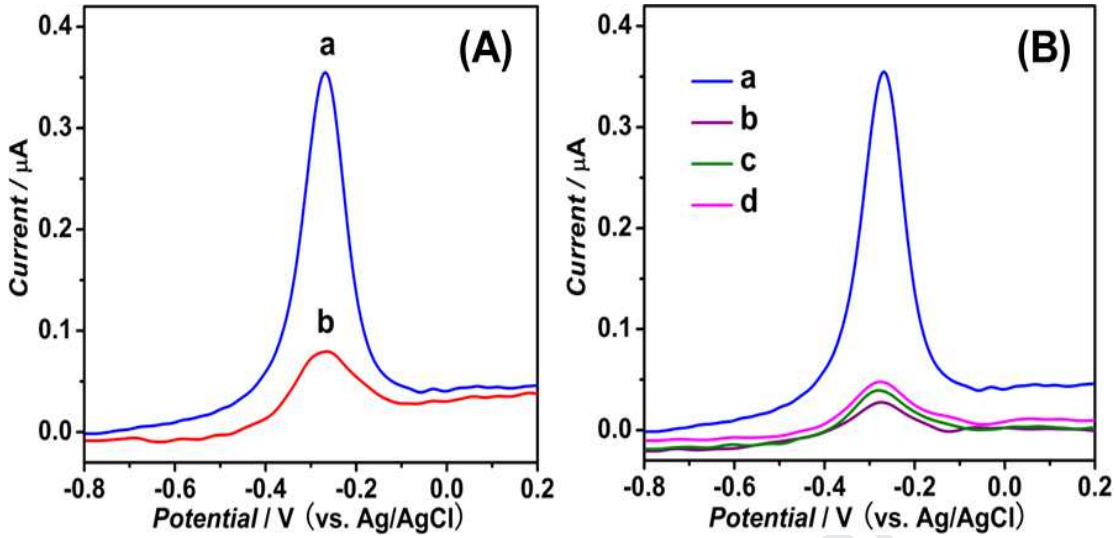

448

449 **Fig. 2**

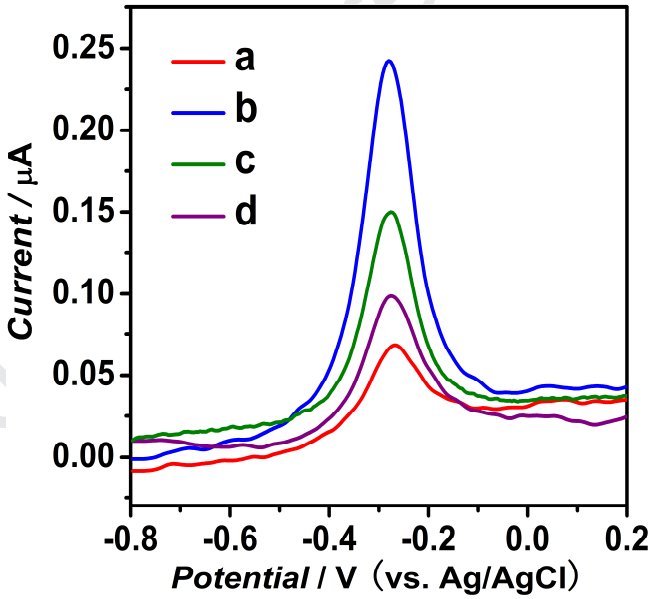

450

451 **Fig. 3**

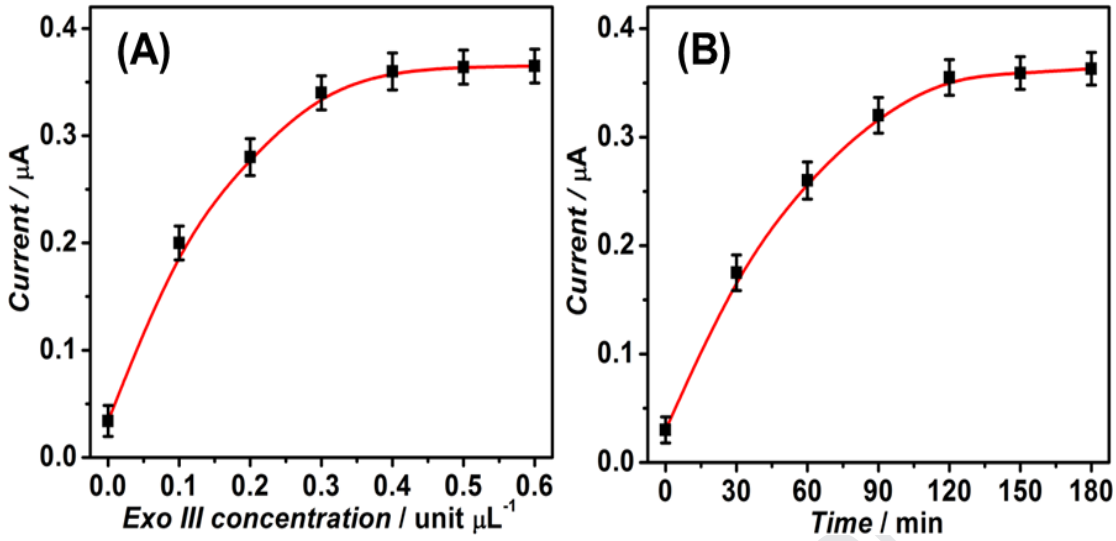
(A)
Current / μA
Exo III concentration / unit μL-1
(B)
Current / μA
Time / min

Fig. 4

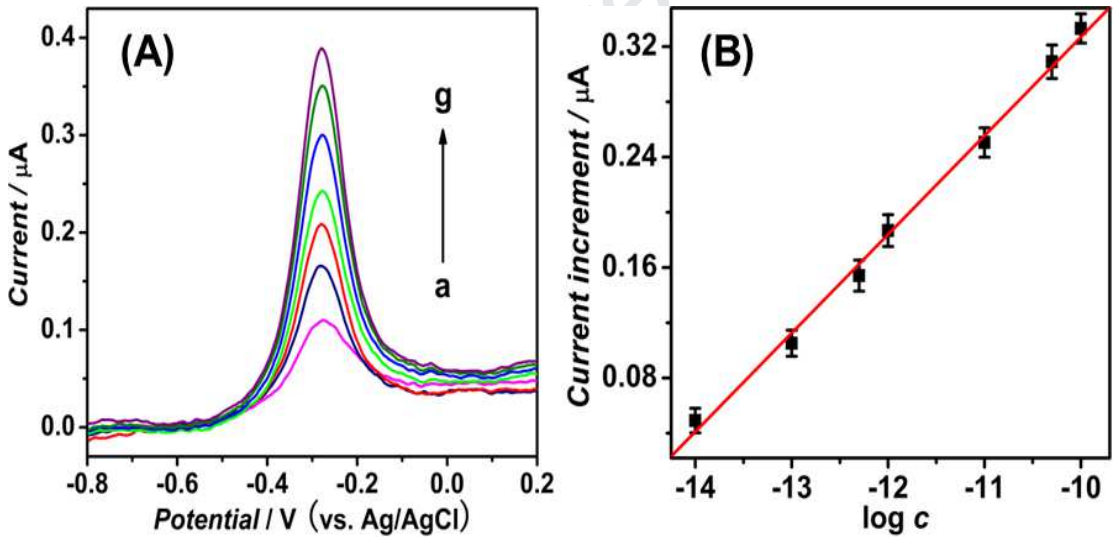
(A)
g
a
Current / μA
Potential / V (vs. Ag/AgCl)
(B)
Current increment / μA
log c

Fig. 5

Highlights

- A signal-on electrochemical biosensor was developed to investigate DNA methylation based on the conformational change of a DNA probe.
- Exo III-assisted signal amplification allowed femtomolar detection of methylated target DNA.
- The proposed method exhibited advantages of convenience, low cost, and high sensitivity.
- This sensing system may be useful for epigenetic evaluation and fundamental biochemistry research.

CRediT authorship contribution statement

Qiumei Feng: Conceptualization, Project administration, Writing - original draft.

Li Qin: Data curation, Methodology.

Mengying Wang: Formal analysis, Validation.

Po Wang: Supervision, Funding acquisition, Writing - review & editing.

Declaration of interests

☒ The authors declare that they have no known competing financial interests or personal relationships that could have appeared to influence the work reported in this paper.

Prof. Po Wang
October 29, 2019

☐The authors declare the following financial interests/personal relationships which may be considered as potential competing interests: